Interaction Notes

Note 193

August 1973

Integral Equation Solution for Induced Surface Currents on Bodies of Revolution

R. A. Perala
Mission Research Corporation

Abstract

The time domain magnetic field integral equation is used to calculate the surface current density caused by an incident plane wave, induced on a fat cylinder. Results that illustrate shadowing on the cylinder are given for two different incident polarizations.

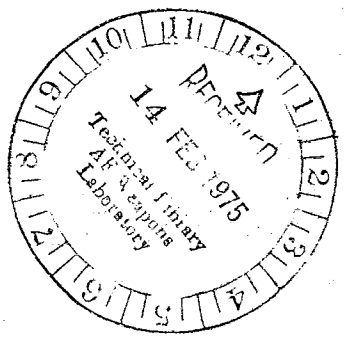

INTEGRAL EQUATION SOLUTION FOR INDUCED SURFACE CURRENTS ON BODIES OF REVOLUTION

I. INTRODUCTION

When a metallic object is illuminated by an electromagnetic wave, surface currents are induced. If the surface has cracks, apertures, or penetrations of some kind, electromagnetic fields will couple into the interior of the metallic object. These penetrating fields can often be defined in terms of the surface current density that exists on the structure if no surface imperfections are present. Thus, if one desires to study the problem of coupling of incident electromagnetic energy to the inside of a metallic body with surface discontinuities, calculation of the surface current densities is important.

The problem addressed in this paper is the calculation of the surface current densities induced on a fat body of revolution by an incident plane wave. Many researchers [1-5] have calculated total currents induced on long, thin cylinders whose length-to-diameter ratios are greater than about 6. Kao [6] has considered scattering from a short, tubular cylinder (no endcaps). In this study, induced current densities are calculated on cylinders whose length-to-diameter ratios are on the order of unity.

The method used employs the time domain magnetic field integral equation (MFIE), following the work of Bennet and Weeks [8], which is also discussed in Poggio and Miller [7]. Bennet and Weeks have applied this method to scattering from cylinders, with the quantity of interest being the scattered far fields.

The quantity of interest here is the surface current density induced on bodies of revolution by an incident plane wave. It is applied specifically to a cylinder with ellipsoidal end caps, although other interesting shapes could be easily studied. Shadowing effects are clearly seen, as the current densities may be calculated equally well on the end caps, illuminated side, or shadowed side of the body.

II. TIME DOMAIN MAGNETIC FIELD INTEGRAL EQUATION (MFIE)

The time domain MFIE used in this study is given in both Poggio and Miller [7] and Bennet and Weeks [8] as

$$\bar{J}_s(\bar{x}_i,t_j) = 2\hat{n}(\bar{x}_i) \times \bar{H}^{inc}(\bar{x}_i,t_j) + \frac{1}{2\pi}\hat{n}(\bar{x}_i) \times \int \left[\frac{1}{c}\frac{\partial}{\partial\tau}\bar{J}_s(\bar{x}',\tau) + \frac{\bar{J}_s(\bar{x}',\tau)}{|\bar{x}_i - \bar{x}'|} \right] \times \frac{(\bar{x}_i - \bar{x}')\, ds'}{|\bar{x}_i - \bar{x}'|^2} \qquad (1)$$

where:

$\bar{x}_i$ = space coordinate of observation point

$\bar{x}'$ = space coordinate of integration point

$\bar{J}_s(\bar{x}_i, t_j)$ = surface current density at space coordinate $\bar{x}_i$ and time coordinate t_j

$\hat{n}(\bar{x}_i)$ = unit normal vector directed outward from the surface

$\bar{H}^{inc}(\bar{x}_i, t_j)$ = incident magnetic field vector that exists if the scatterer is not present

$\tau = t_j - \frac{|\bar{x}_i - \bar{x}'|}{c}$, retarded time

c = speed of light

ds' = differential surface area.

Also, the principal value of the integral, indicated by $\int\!\!\!\!\!\!-$, means that the integration does not include the elemental area surrounding the singular point $\bar{x}_i = \bar{x}'$.

By inspection of (1), it is obvious that the surface current at a time t_j is the sum of two terms. The first term on the right-hand side of (1) may be regarded as a "source" term. It involves only $\hat{n}(\bar{x}_i)$ (which is known for a particular body) and the incident magnetic field (which is a known input to the problem). Therefore, this whole term involves functions that are given in the statement of the problem, and is quite simply calculated.

The second term involves the surface integral over the body. The integrand contains a term involving the value of the surface current and its time derivative at some past time, namely $t_j - \frac{|\bar{x}_i - \bar{x}'|}{c}$.

If it is assumed that the surface current at past times has already been calculated, then the whole integral involves known functions. Therefore, the surface current $\bar{J}(\bar{x}_i, t_j)$ is completely specified in terms of known quantities.

III. NUMERICAL SOLUTION OF THE MFIE

A computer code has been written which solves equation (1) for a given body of revolution. A body of revolution is defined as the body generated by a curve $\rho(z)$ as it is rotated about the z axis. The inputs required for the code are $\rho(z)$, $\frac{\partial \rho(z)}{\partial z}$, $\bar{H}^{inc}(\bar{x}_i, t_j)$, and inputs relating to the time and space intervals desired for the numerical solution.

In cylindrical coordinates, the differential area is given by

$$ds' = \sqrt{1 + \left(\frac{\partial \rho(z)}{\partial z}\right)^2}\ \rho(z)\ dz d\phi \quad . \tag{2}$$

and the unit normal is given by

$$\hat{n}(z,\phi) = \left(\hat{u}_\rho - \frac{\partial \rho(z)}{\partial z}\,\hat{u}_z\right) \Big/ \sqrt{1 + \left(\frac{\partial \rho(z)}{\partial z}\right)^2} \quad . \tag{3}$$

The integrand of the surface integral in (1) is evaluated in rectangular coordinates, since this coordinate system does not depend upon the location of the integration point.

Since in the numerical solution the time values t_j are necessarily discrete, the values of the surface current are only computed at discrete time values. The surface integral, however, involves values of the surface currents at a retarded time τ, which in general does not correspond to any discrete time value. To overcome this difficulty, a

parabolic (second order) curve fit [9] is used to evaluate the surface current at the retarded time. The time derivative of the surface current is obtained by analytically differentiating the second order polynomial approximation. The code is set up in such a way that the discrete time point at the center of the polynomial fit is set as close to the retarded time τ as is possible, thereby insuring that the surface current and its time derivative are evaluated as close to the center of the polynomial fit as possible.

The surface integral is evaluated by the rectangular rule. That is, the surface is broken up into a number of patches according to a segmention scheme in z and ϕ. The integrand is evaluated at the center of a given patch, and its contribution to the integral is obtained by multiplying the integrand evaluated at the center of the patch by the area of the patch. The integration is thus replaced by a summation. The principal value of the integral is obtained by numerically skipping the evaluation of the integrand over the self patch, i.e., where $\overline{x}_i = \overline{x}'$.

The solution proceeds as follows. It is assumed that at $t_j = 0$, the incident field has not yet arrived and, therefore, all of the surface currents are zero. At $t_j = \Delta t$ (where Δt is the time interval), it is assumed that the incident wave arrives on the body, and then the surface current depends only on the source term, and the contribution from the integral is zero. This is because the integral depends

upon surface current values of past times, all of which are zero. At $t_j = 2\Delta t$, the surface current then depends upon both the source term and the surface integral, because there now are values of the surface currents for past times. The solution then proceeds in the same manner up to the desired end point in time.

Although in general the surface current density has 3 vector components, it is necessary to find only the ϕ and either the z or ρ components, because the other one can be found from

$$\hat{n}(\bar{x}_i) \cdot \bar{J}(\bar{x}_i, t_j) = 0 \ , \tag{4}$$

which yields

$$\bar{J}_\rho(\bar{x}_i, t_j) = \bar{J}_z(\bar{x}_i, t_j) \frac{\partial \rho(z)}{\partial z} \ . \tag{5}$$

IV. NUMERICAL RESULTS

In order to demonstrate the accuracy of the code, a comparison was made with known results for a plane wave incident on a sphere. Figure 1 shows the coordinate system and geometry used for a fat cylinder. In terms of the notation of Figure 1, a sphere was defined as a fat cylinder of half-height h = 0, and with the end caps as hemispheres of radius a = 1. The surface current component in the ϕ direction was calculated at $\phi = 135°$ and z = 0, and compared with the result given in reference 10 at the same location. Figure 2 shows the comparison. The excitation for Figure 2a (Reference 10) is a unit step plane wave traveling in the negative x direction, with the E field directed in the negative y direction. The excitation for Figure 2b is also a unit step except that the leading edge

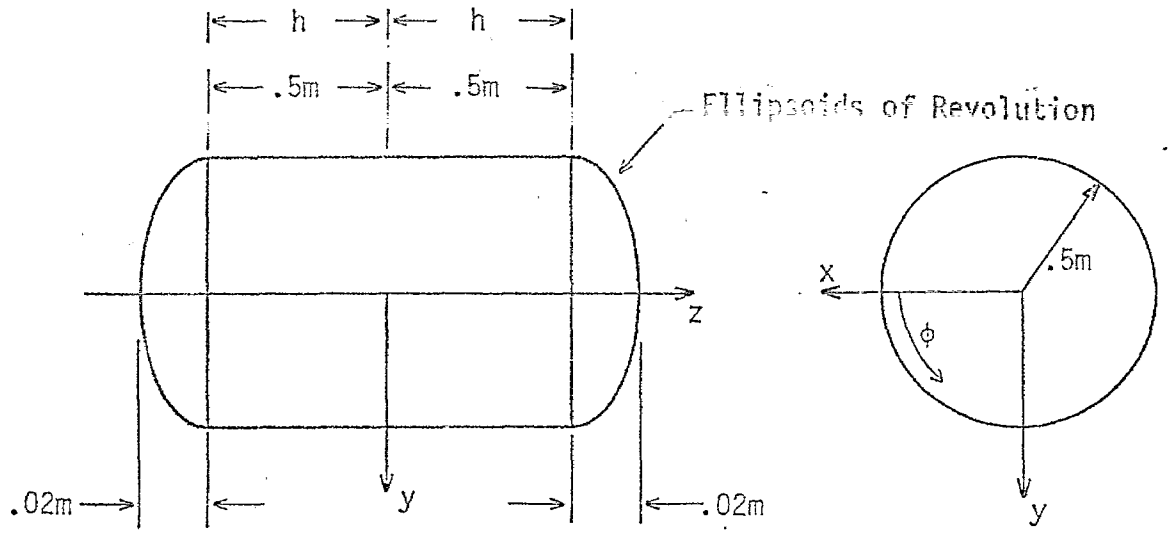

Figure 1. Fat Cylinder Diagram and Coordinate System.

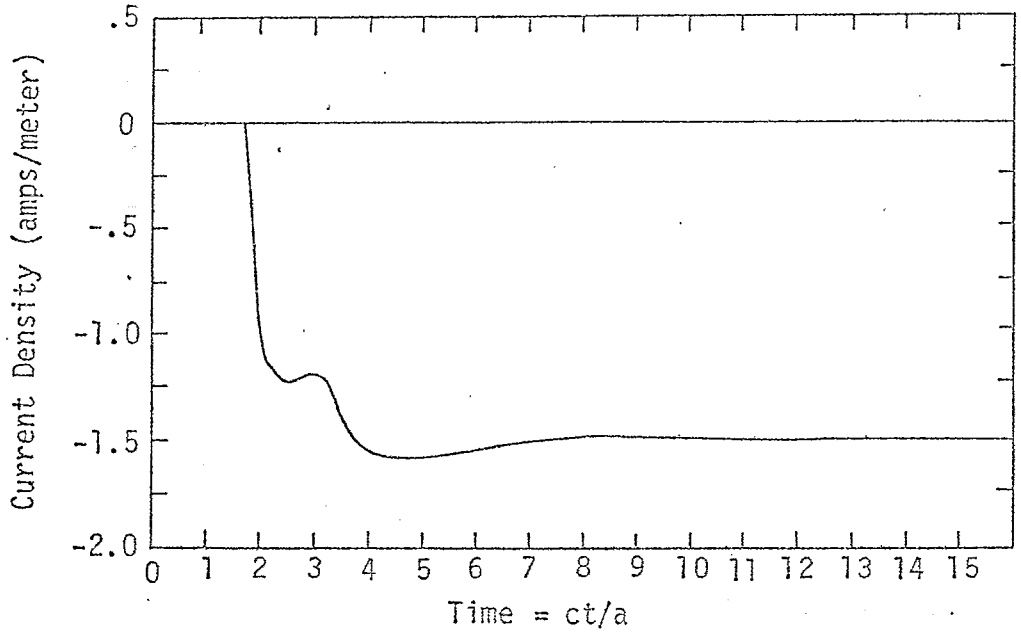

a. J_ϕ obtained from Reference 10

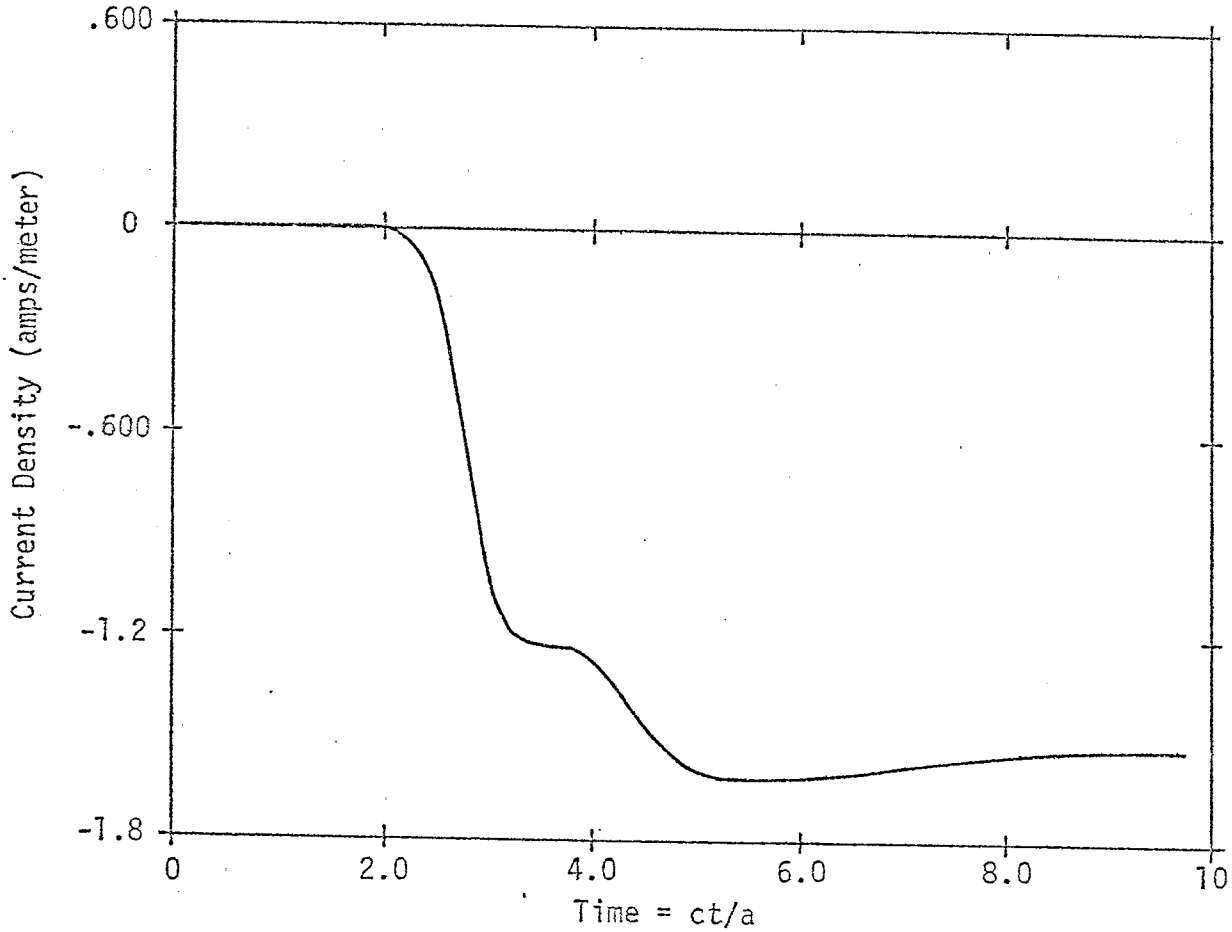

b. J_ϕ obtained by the MFIE

Figure 2. Comparison of MFIE Technique With that of Reference 10, at $\phi = 135°$, $z = 0$

is replaced by the leading edge of a gaussian pulse which is described below. This gaussian pulse which has a risetime of about 2 nanoseconds was used because the MFIE solution was unstable for a perfect unit step input. Thus, the only difference between the two curves is in the high frequency content, and is caused by the longer risetime of the input for Figure 2b.

The next shape studied was the cylinder shown in Figure 1, with its coordinate system. As can be seen, the half height equals the radius of .5 meters. The end caps are ellipsoids of revolution, whose semi-major axis is the cylinder radius, and whose semi-minor axis is .02 meters. Two cases of incident polarization are considered. In both cases, the incident wave is a gaussian pulse traveling in the negative $\bar{x}$ direction, which for unit peak amplitude is given by $f(\bar{x},t) = \exp\left(-3.6\times10^{17}\left(t + \frac{(x-1.8)}{c}\right)^2\right)$. The first case considers an incident field such that the electric field is in the positive z direction with a peak amplitude of 377 V/m. This corresponds to the incident magnetic field in the y direction and having a peak amplitude of 1 a/m. The second case considers an incident field such that the electric field is in the negative y direction, and is, therefore, perpendicular to the cylinder axis. It is also a gaussian pulse with peak amplitude of 377 V/m. The magnetic field is in the positive z direction with a peak amplitude of 1 a/m.

The segmentation scheme used was as follows, Each of the end caps was divided into three equal segments in z. The main cylinder body was divided into 6 equal segments in z. The entire body was uniformly segmented into 18 segments in ϕ.

The surface currents were calculated in the time domain, and the Fourier transform taken to obtain frequency domain response. The Fourier transform is defined as

$$F(w) = \int_{-\infty}^{\infty} f(t)e^{-jwt}dt \quad . \tag{6}$$

This transform was then divided by the Fourier transform of the input gaussian pulse, yielding the system transfer function (impulse response) in the frequency domain. These transfer function magnitudes are plotted in Figures 3 and 5 for the two polarizations. Figures 4 and 6 show the variations of the time domain response with coordinates z/h and ϕ of Figure 1. These plots show the absolute value of the largest half cycle of the time domain response as a function of ϕ (to illustrate shadowing) and z/h. Typical time domain waveforms are shown in Figures 3s and t, and in Figures 5s and t for the two different polarizations. Although these time domain waveforms have been truncated to show the early time history of the response, the time domain solution proceeded until the surface current densities decayed to zero, thus ensuring the accuracy of the Fourier transform in the low frequency regime. The surface currents stabilize and decay to zero rapidly, normally much before ct/h = 18. The time step was $2\text{x}10^{-10}$ seconds, and thus less than 150 time steps were required until the surface current densities decayed to zero. Trial runs were made with varying degrees of segmentation in both time and space until the solution converged, thus ensuring that numerical error was minimized.

Symmetry considerations should be noted. It is observed that for the incident wave polarized parallel to the z axis, that $J_z(z,\phi,t)$ is an even function of z and ϕ, while $J_\phi(z,\phi,t)$ is an odd function of both z

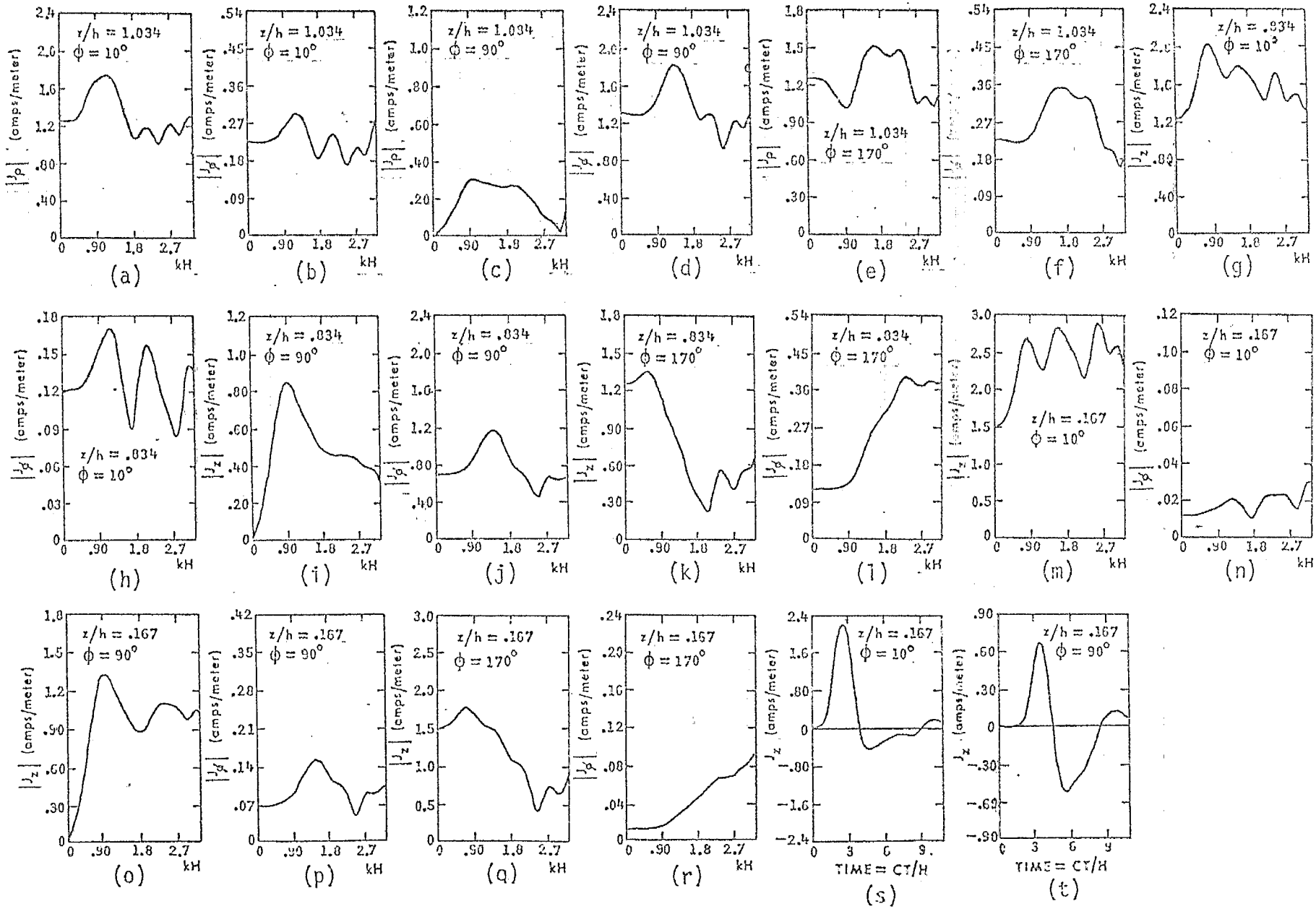

Figure 3. a-r: magnitude of CW transfer function at various cylinder coordinates.
s-t: time domain response to unit amplitude gaussian pulse.
Polarization parallel to z axis.

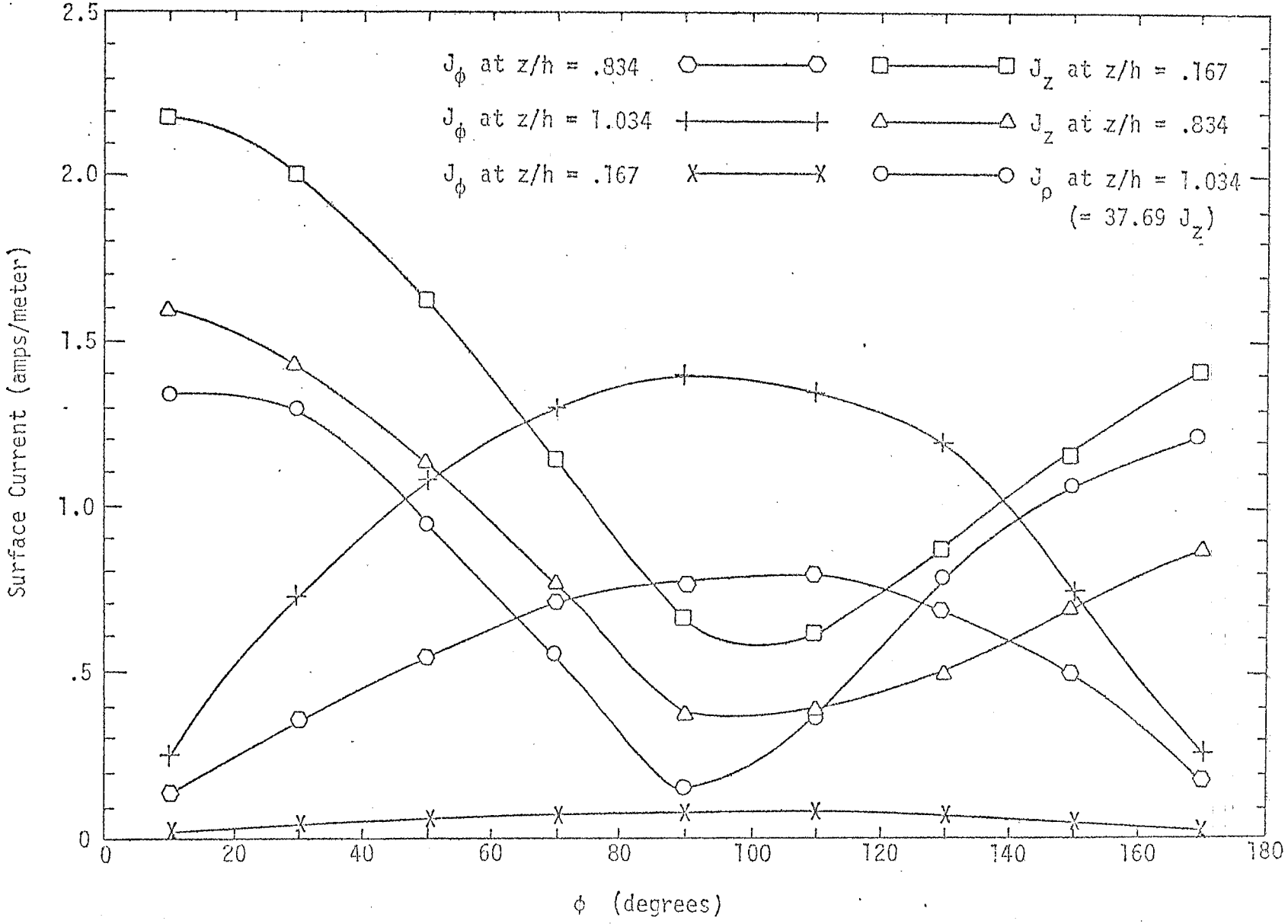

Figure 4. Variations of Surface Current Peak Amplitudes With ϕ and z. Incident Field Polarized Parallel to z Axis.

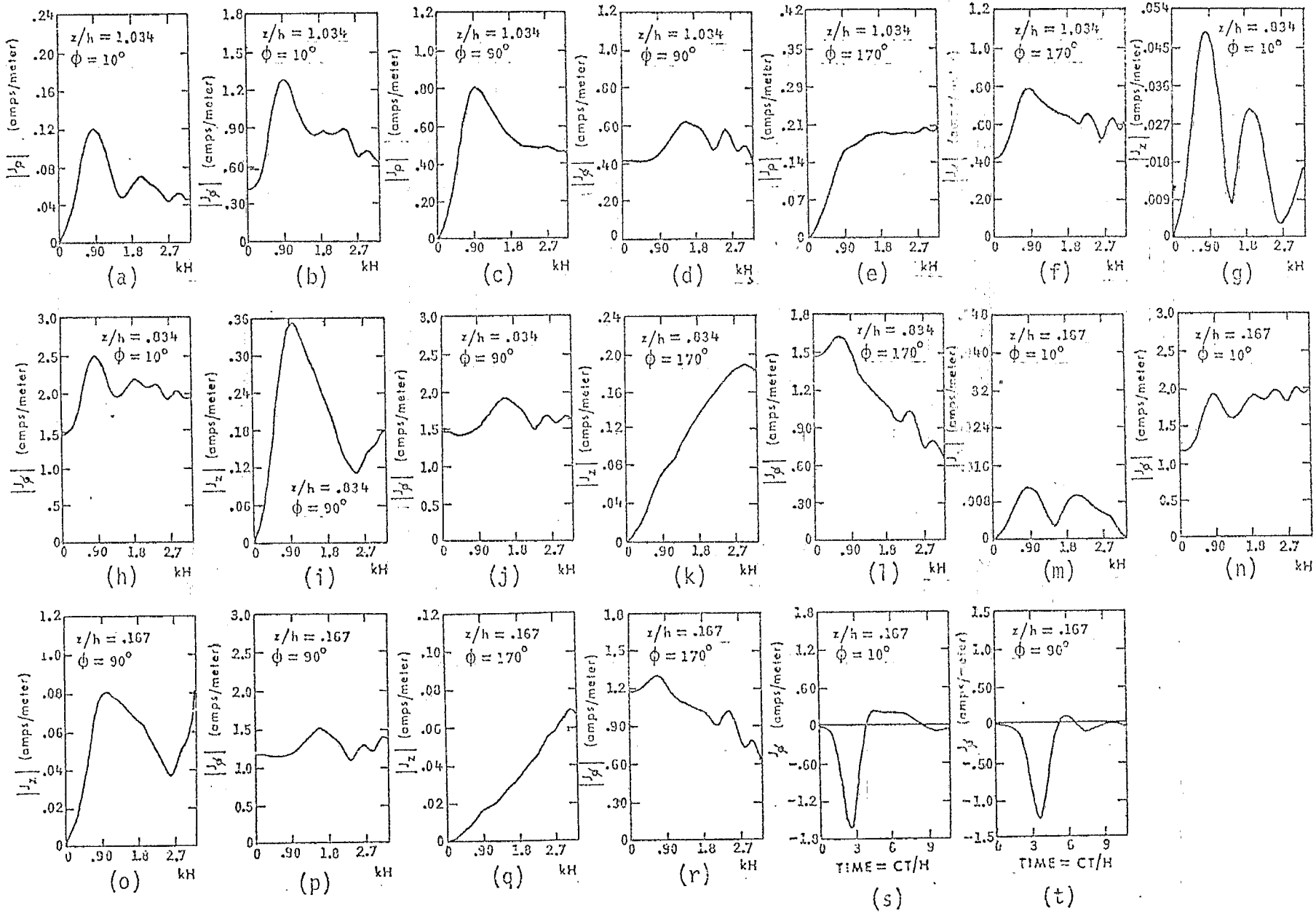

Figure 5. a-r: magnitude of CW transfer function at various cylinder coordinates.
s-t: time domain response to unit amplitude gaussian pulse.
Polarization perpendicular to z axis.

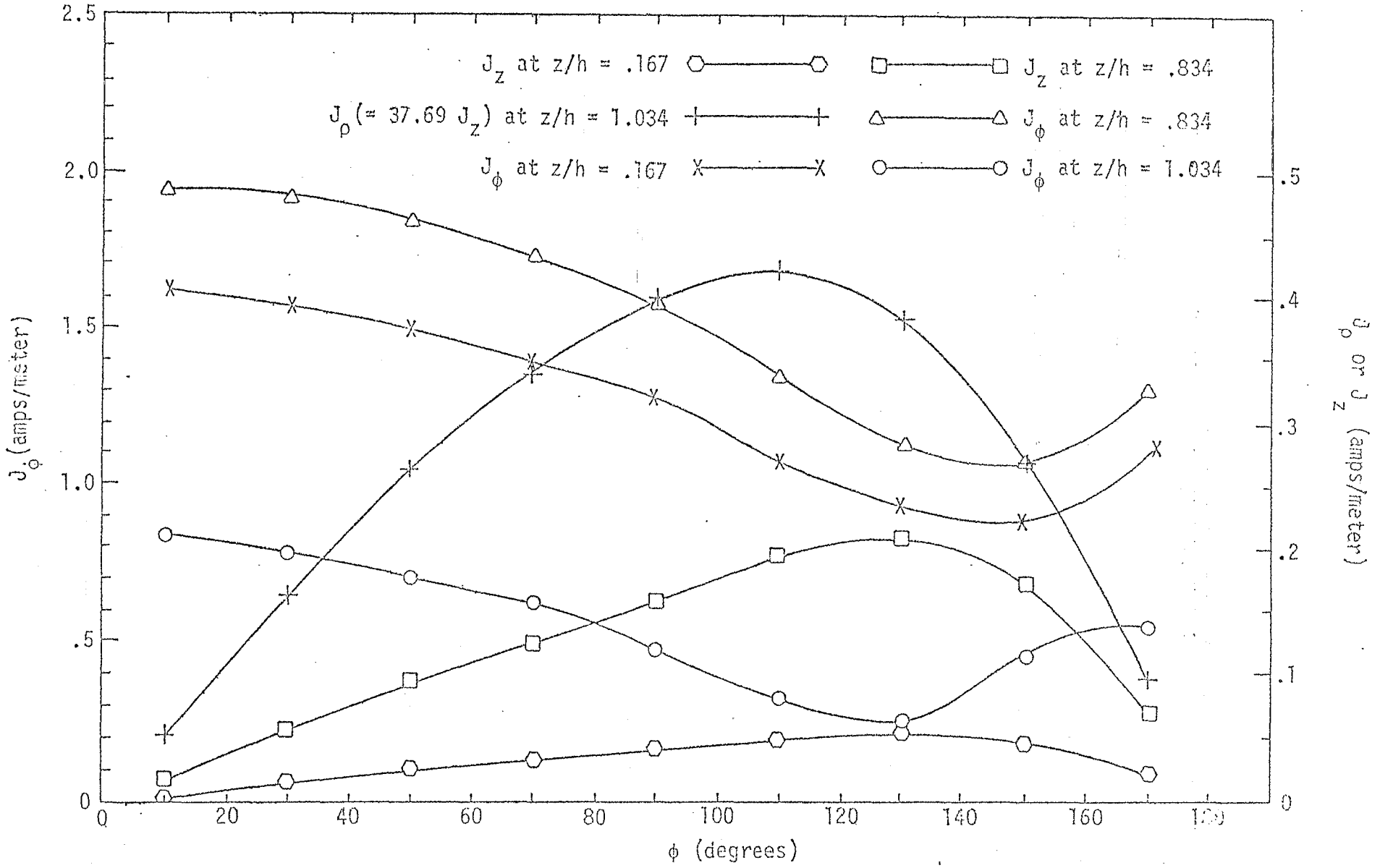

Figure 6. Variations of surface current peak amplitudes with ϕ and z. Incident field polarized perpendicularly to z axis.

and ϕ, while $J_\phi(z,\phi,t)$ is an even function of both z and ϕ. Of course, for both polarizations, the magnitudes of the CW response for both current components are even functions of both ϕ and z.

It should also be noted with regard to Figures 3 to 6, that for the location given on the end cap (z/h = 1.034) the z-component of the current is not given since at this location $|J_\rho| = 37.69\ |J_z|$.

REFERENCES

1. Sassman, R. W., The Current Induced on a Finite, Perfectly Conducting, Solid Cylinder in Free Space by an Electromagnetic Pulse, Northrop Corporate Laboratories, July 1967, EMP Interaction Note 11.

2. Harrison, Charles W., Jr., Missile Circumferential Current Density for Plane Wave Electromagnetic Field Illumination, Sandia Report Number SC-R-70-4324, 30 July 1970, EMP Interaction Note 60.

3. Barnes, 1Lt. Paul R., The Axial Current Induced on an Infinitely Long, Perfectly Conducting, Circular Cylinder in Free Space by a Transient Electromagnetic Plane Wave, Air Force Weapons Lab., March 1971, EMP Interaction Note 64.

4. Merewether, David E., Transient Currents Induced on a Metallic Body of Revolution by an Electromagnetic Pulse, Sandia Report SC-R-71-3213, May 1971, EMP Interaction Note 93.

5. Sancer, M. I., and A. D. Varvatsis, Calculation of the Induced Surface Current Density on a Perfectly Conducting Body of Revolution, Northrop Corporate Laboratories, April 1972, EMP Interaction Note 101.

6. Kao, Cheng C., Electromagnetic Scattering from a Finite Tubular Cylinder: Numerical Solutions and Data, I. "Development of Theory", AFCRL-69-0535(1), Contract F19628-68-C-0030, December 1969. This report contains a complete program in Fortran 4 for the IBM 360/65 for computing the inside and outside current densities and the total current density, among other things.

7. Poggio, A. J., and E. K. Miller, "Integral Equation Solutions of Three-Dimensional Scattering Problems," Numerical Techniques for Antennas and Electromagnetics, Vol. II, University of Southern California, June 1973.

8. Bennett, C. L. and W. L. Weeks, "Electromagnetic Pulse Response of Cylindrical Scatterers," G-AP Symposium, Boston, Mass., 1968. See also A Technique for Computing Approximate Electromagnetic Impulse Response of Conducting Bodies, Purdue University Report TR-EE68-11.

9. Crandall, S. H., Engineering Analysis, McGraw-Hill, p. 155, 1956.

10. Martinez, Joe P., Zoe Lynda Pine, and F. M. Tesche, Numerical Results of the Singularity Expansion Method as Applied to a Plane Wave Incident on a Perfectly Conducting Sphere, Dikewood Corporation, May 1972, EMP Interaction Note 112.